Tight-Binding Parametrization for Photonic Band Gap Materials

E. Lidorikis,[1] M. M. Sigalas,[1] E. N. Economou,[2] and C. M. Soukoulis[1,2]
[1]*Ames Laboratory–U.S. DOE and Department of Physics and Astronomy, Iowa State University, Ames, Iowa 50011*
[2]*Research Center of Crete-FORTH and Department of Physics, University of Crete, Heraklio, Crete 71110, Greece*
(Received 10 March 1998)

The idea of the linear combination of atomic orbitals method, well known from the study of electrons, is extended to the classical wave case. The Mie resonances of the isolated scatterer in the classical wave case are analogous to the atomic orbitals in the electronic case. The matrix elements of the two-dimensional tight-binding (TB) Hamiltonian are obtained by fitting to *ab initio* results. The transferability of the TB model is tested by reproducing accurately the band structure of different 2D lattices, with and without defects, and at two different dielectric contrasts. [S0031-9007(98)06889-6]

PACS numbers: 42.70.Qs, 41.20.Jb, 71.15.–m

In recent years experimental and theoretical studies of artificially manufactured periodic dielectric media called photonic band gap (PBG) materials or photonic crystals have attracted considerable attention [1,2]. PBG materials can have a profound impact in many areas in pure and applied physics. PBG materials are often considered as analogous to electronic semiconductors. The existence of spectral gaps in periodic PBG materials or localized states in disordered systems, in analogy with what happens to the electronic materials, is of fundamental importance. Two different mechanisms, single scatterer resonances and macroscopic Bragg-like multiple scattering, contribute to the formation of gaps and localized states. Preliminary results [3,4] have shown that there is a direct correspondence between the gaps calculated by plane wave expansion and the Mie resonances [5] of an isolated sphere. It is surprising that the positions of the Mie resonances approximately coincide with the center of the bands. It is tempting to suggest that the Mie resonances of an isolated scatterer play the role of the energy levels of an isolated atom in a crystal. This opens up the possibility to formulate the problem in a simpler way, similar to the tight-binding (TB) formulation of the electronic problem.

It is well known that the TB method has proven to be very useful in studying the electronic properties of solids [6–9]. In an empirical TB approach, matrix elements of the Hamiltonian between orbitals centered on different sites are treated as parameters which are adjusted to obtain the band structure and the band gaps, which have been determined by other more accurate methods. The parameters obtained in this way are then used to study other properties of the systems, such as surface states, impurities, and properties of disordered systems. The success of the TB formulation has been tested in the studies of all kinds of materials including Si, C, and hydrogenated amorphous systems [7–10].

In this paper, we show that it is possible to extend the ideas of the linear combination of atomic orbitals (LCAO) method to the classical wave case. The Mie resonances of the isolated scatterer in the classical case play the same role as the atomic orbitals in the electronic case. However, there exist two important differences. First, Mie resonances' states are not localized; in fact, they decay too slowly, as $1/r$ as $r \to \infty$, and this may lead to divergences in some matrix elements. However, in a lattice environment they may be taken as localized, with a localization length comparable to the interparticle dimension. Second, in the classical wave case, as opposed to the electronic case, the host medium supports propagating solutions for every frequency. For large wavelengths, this is the dominant propagation mode since no resonances have been excited yet, while for wavelengths comparable to the particle dimension, transmission is achieved mainly through transfer between neighboring localized resonances. Thus, we may assume that the lowest frequency band is plane wavelike, while the higher bands are TB-like. This picture is more easily justified in the case of wide gaps and narrow bands, but its validity seems to be much wider. Within the framework of the systems we studied, we verified this picture. Furthermore, we were able to show that the TB matrix elements, after an appropriate rescaling, are functions of the distance only.

We will consider the scalar case of a 2D periodic array of N infinitely long dielectric cylinders in vacuum, with periodic boundary conditions and with the incident plane wave E polarized. We assume the normalized electric field for each band to be given by

$$E_n(\vec{r},\vec{k}) = \frac{c_n^1(k)}{\sqrt{N}}\, e^{i\vec{k}\vec{r}} + \frac{c_n^2(k)}{\sqrt{N}} \sum_{\vec{R}} \Psi_n(\vec{r} - \vec{R}) e^{i\vec{k}\vec{R}}, \tag{1}$$

where $n = 0, 1, 2, \ldots$ is the band's index and $\Psi_n(\vec{r} - \vec{R})$ with an angular symmetry $\Psi \sim \cos(n\theta)$ stands for the wave function of the nth resonance localized at $\vec{R}$. $c_n^1 = 0$, $c_n^2 = 1$ for $n \neq 0$, and are functions of the frequency ($k \equiv |\vec{k}|$) only for $n = 0$ with $|c_0^1|^2 + |c_0^2|^2 = 1$. $\vec{r}$, $\vec{R}$, $\vec{k}$ are 2D vectors, and we have assumed a unit area unit cell. In order to simplify the problem and make a better correspondence with the electronic case, we take the Ψ_n's to be orthonormal to each other and orthogonal to e^{ikr} so that $\int E_m^* E_n \, d\vec{r} = \delta_{mn}$. This will turn out to be a good approximation for our case. For the lowest frequency

band, we should expect $c_0^1 \to 1, c_0^2 \to 0$ for $|\vec{k}| \to 0$ and $c_0^1 \to 0, c_0^2 \to 1$ for $|\vec{k}| \to |\vec{G}|/2$.

The "Hamiltonian" for the scalar wave equation is $H = -\vec{\nabla}^2/\epsilon(\vec{r})$ and the eigenfrequencies ω^2/c^2 of the system can be found by diagonalizing the Hamiltonian matrix $H_{mn} = \int E_m^* H E_n \, d\vec{r}$. For a square lattice with lattice constant a, using the standard notation [6–8] and taking up to second nearest neighbors into account, the H_{00} matrix element will be

$$H_{00} = |c_0^1|^2 |k|^2/\langle\epsilon\rangle + |c_0^2|^2 \times [\varepsilon_s + 2V_{ss\sigma}^{(1)}(\cos\phi_x + \cos\phi_y) + 4V_{ss\sigma}^{(2)} \cos\phi_x \cos\phi_y], \quad (2)$$

where $\phi_x = k_x a$, $\phi_y = k_y a$, $|k| = \sqrt{k_x^2 + k_y^2}$, $\langle\epsilon\rangle$ is the average dielectric constant, $\varepsilon_s = \int \Psi_0^*(\vec{r}) H \Psi_0(\vec{r}) \, d\vec{r}$, and $V_{ss\sigma}^{(1),(2)} = \int \Psi_0^*(\vec{r}) H \Psi_0(\vec{r} - \vec{R}^{(1),(2)}) \, d\vec{r}$; the superscripts (1) and (2) stand for first and second neighbors. We argue that the functional form of $|c_0^2(k)|^2$ is similar to the form of the scattering cross section of a single cylinder [5] for the $n = 0$ (or s-wave) case, so that $|c_0^1(k)|^2 \simeq e^{-\lambda(f)\omega_r^\mu}$. Here $\omega_r = |\vec{k}|c/(\omega_0\sqrt{\langle\epsilon\rangle})$, ω_0 is the single cylinder Mie resonance frequency, $\lambda(f)$ is a function of the filling ratio f of the form $\lambda(f) = h_1/f^{h_2}$. The exponent μ has to be larger than 2 in order to preserve the correct slope at $|\vec{k}| \to 0$. For simplicity, we choose $\mu = 4$.

The second band ($n = 1$ or p-like) has a $\Psi \sim \cos\theta$ symmetry, and will consist of two linearly independent polarizations, p_x and p_y. The Hamiltonian matrix elements are

$$H_{p_x p_x} = \varepsilon_{p_x} + 2V_{pp\pi}^{(1)} \cos\phi_y + 2V_{pp\sigma}^{(1)} \cos\phi_x + 2(V_{pp\sigma}^{(2)} + V_{pp\pi}^{(2)}) \cos\phi_x \cos\phi_y, \quad (3)$$

$$H_{p_x p_y} = 2(V_{pp\pi}^{(2)} - V_{pp\sigma}^{(2)}) \sin\phi_x \sin\phi_y, \quad (4)$$

where all quantities are defined the same way as in Eq. (2). The matrix element $H_{p_y p_y}$ is similar to $H_{p_x p_x}$ with $x \leftrightarrow y$; $H_{p_y p_x} = H_{p_x p_y}^*$. In this Letter we consider only these two bands. We take also the dielectric constant of the cylinders to be $\epsilon = 100$. This large value of ϵ ensures that the matrix element H_{sp} is negligible. However, even smaller values of ϵ (e.g., $\epsilon = 13$) seem to give $H_{sp} \simeq 0$.

We have fitted the V and ε matrix elements, as well as the value of λ, to the band structure of five different rectangular lattices with large/small axis ratios: $1, 1.05, 1.1, 1.15, 1.2$ as well as to a hexagonal lattice, for six different filling ratios: $f = 0.1$–0.6. Taking into account up to third nearest neighbors for the rectangular lattice involves 13 (9 V's, 3 ε's, and the value of λ) adjustable parameters, while for the hexagonal we considered only first nearest neighbors and so used only 6 adjustable parameters. The quality of these fits can be seen in Fig. 1 where we plot the bands as found numerically by the plane wave expansion (PWE) method along with the TB fit, for a square and a hexagonal lattice for two filling ratios. The excellent fit is an indication of the potential usefulness of the TB method.

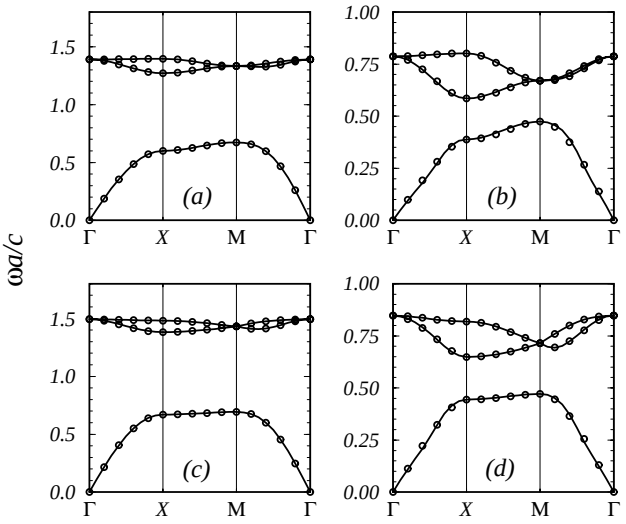

FIG. 1. The first two frequency bands for a square lattice with filling ratio $f = 0.1$ (a) and $f = 0.4$ (b), and for a hexagonal lattice with $f = 0.1$ (c) and $f = 0.4$ (d). Circles correspond to numerical results from the PWE method, while solid lines correspond to the TB fit.

We plot next some of the fitted matrix elements. The square root of the diagonal ε_{p_x} and ε_{p_y} matrix elements are plotted [Fig. 2(a)] as a function of the filling ratio f, while the off-diagonal $V_{pp\pi}$ matrix elements are plotted [Fig. 2(c)] as a function of the dimensionless separation distance $d_{ij} = r_{ij}/\alpha$, where r_{ij} is the separation distance between cylinders i and j and α is the cylinders' radius. Obviously the matrix elements, especially $V_{pp\pi}$, do not depend on a single parameter (e.g., d_{ij}). Apparently the lattice environment [10] has to be included, hopefully through rescaling functions.

The proposed simple rescaling function $(D_n^{\rm on})_i$ for the diagonal matrix elements of cylinder i that takes into account the filling ratio and the different symmetries is of the form

$$\frac{1}{(D_n^{\rm on})_i} = \sum_{j \neq i} \frac{\tau \cos^2(n\theta_{ij})}{d_{ij}^{\nu_n}}, \quad (5)$$

where θ_{ij} is the angle between the symmetry axis of the p resonance on cylinder i and the $\hat{r}_{ij}$ direction, $n = 0, 1, \ldots$, for the s, $p, \ldots$, resonances, and the sum runs over the nearest neighbors of cylinder i. The power on the angular function was chosen so that the p_x and p_y resonances in the hexagonal lattice are the same. The only choices were 2 and 4, and it was found that 2 gives better results. Equation (5) is similar to what was used in Ref. [10] for the atomic orbitals, except for two differences: (a) Here we take into account the resonance's angular symmetry, and (b) the exponentially decaying part is missing, reflecting the nonlocalized character of the

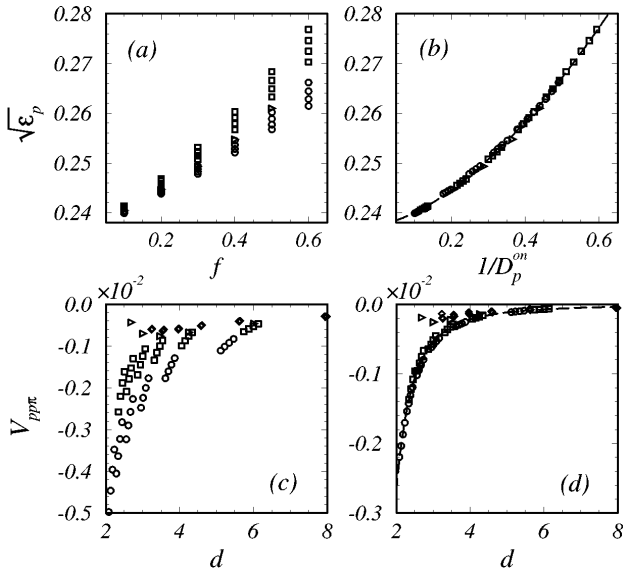

FIG. 2. Fitted TB parameters for the second (p-like) frequency band. (a) $\sqrt{\varepsilon_p}$ vs f. (b) $\sqrt{\varepsilon_p}$ vs the rescaled environment function $1/D_p^{\rm on}$. Circles and squares correspond to $\sqrt{\varepsilon_{p_x}}$ and $\sqrt{\varepsilon_{p_y}}$, respectively, of a rectangular lattice with the big axis along $\hat{x}$, and triangles to a hexagonal lattice. (c) $V_{pp\pi}$ vs the dimensionless separation d. (d) The rescaled $\mathcal{V}_{pp\pi}$ vs d. Circles, squares, and diamonds correspond to a rectangular lattice's $V_{pp\pi}$ elements along the small axis, the large axis, and the diagonal, and triangles to a hexagonal lattice. All matrix elements are expressed in the dimensionless units of $(\omega\alpha/c)^2$.

EM resonances. Finally, $\tau = [\pi\alpha^2/(a^2 f)]^2$ takes into account that different structures, with the same a and α, have different filling ratios. $\tau = 1$ for the rectangular structures and $\tau = 3/4$ for the hexagonal. We will use this parameter only for the diagonal matrix elements.

For the periodic case, the function $(D_n^{\rm on})_i$ is the same for every i. We find that the diagonal matrix element depends on $(D_n^{\rm on})_i$ as follows: $\sqrt{\varepsilon_n} = a_0^n + a_1^n (D_n^{\rm on})^{-a_2^n} + a_3^n (D_n^{\rm on})^{-a_4^n}$ where $a_0^n = \omega_0\alpha/c$ is the corresponding dimensionless Mie resonance frequency and the a_j^n's ($j = 1, \ldots, 4$) are constants. In Fig. 2(b) we plot $\sqrt{\varepsilon_p}$ vs the environment function $(1/D_p^{\rm on})$. We can see that $\sqrt{\varepsilon_p}$ now scales very well, having a larger value for increasing lattice density. The same dependence is found for all bands.

In order to rescale the off-diagonal V matrix element between two neighboring resonances i and j, we need contributions from the neighbors that are close to the line joining i and j. Contributions have to be projected on the $\hat{r}_{ij}$ direction for the s resonance, while for the p resonance we have to project on its symmetry axis. Only first nearest neighbors will contribute. At the end, we have to normalize with the sum of all projection weights.

A simple formula that describes the environment of the n resonance on cylinder i along the $\hat{r}_{ij}$ direction is

$$\frac{1}{(D_n^{\rm off})_{ij}} = \frac{\sum_l (\cos^2\theta_{ilj}^n / d_{il}^{\nu_n})}{\sum_l \cos^2\theta_{ilj}^n}, \qquad (6)$$

where l runs over i's nearest neighbors (including j). θ_{ilj}^n is the angle between the $\hat{r}_{il}$ and $\hat{r}_{ij}$ directions for the s resonance ($n = 0$), and for the p resonance ($n = 1$), it is the angle between the ith resonance's symmetry axis and the $\hat{r}_{il}$ direction. Both angles are taken to have a range from $-\pi/2$ to $\pi/2$ [11]. Finally, if we include screening in our considerations, then the actual matrix element V to be used in a particular problem can be obtained by the fully rescaled one $\mathcal{V}$, by $V^{ij} = \mathcal{V}^{ij}(1 - S^{ij})/[(D^{\rm off})_{ij}^{-1} + (D^{\rm off})_{ji}^{-1}]$ where S^{ij} is the same screening function used in Ref. [10]: $S^{ij} = \tanh(b_1 \sum_{l\neq i,j} e^{-b_2[(d_{il}+d_{jl})/d_{ij}]^{b_3}})$, and is different for different matrix elements. The fully rescaled matrix elements are found to scale with separation distance as $\mathcal{V}^{ij} = c_1 d_{ij}^{-c_2} + c_3 d_{ij}^{-c_4}$ where $c_1, \ldots, c_4$ are constants. In Fig. 2(d) we plot the rescaled $\mathcal{V}_{pp\pi}$ matrix element. We see now that it is a smooth function of separation distance, except for the third nearest neighbor matrix elements which do not scale very well for large filling ratios (small distances). Apparently an improved screening function that depends on the filling ratio as well is needed.

The constants in the expressions for the ε's and the $\mathcal{V}$'s are given in Tables I and II. We have also found $\nu_n = 1.65$ for all n, and $h_1 = 0.068$, $h_2 = 1.23$ for $\lambda(f)$.

To check the transferability of our results we study first the defect case shown in the inset graph of Fig. 3(a). There the central cylinder of a 3×3 supercell is displaced as shown. For $\vec{k}a = (0, 1/3)$ we plot in Fig. 3(a) the three edge eigenfrequencies of the first two bands, and directly compare our results with the ones obtained numerically by the PWE method for exactly the same system. The agreement is excellent. Thus our TB parametrization works very well for the defect case too. It is worth noting that the PWE method takes a factor of 10^4 more CPU time than the TB method.

The second test checks the transferability of our parameters for different dielectric contrasts. We fitted the TB parameters for a square lattice of $\epsilon = 13$ for 5 different filling ratios. The quality of the fit can be seen in Fig. 3(b) where we plot the PWE bands along with the TB fit for the $f = 20\%$ case. We find that the matrix elements are rescaled by the same functions with the same parameters except for only a different power ν, and scale with distance with the same c parameters as obtained from Table II, except for a multiplication constant. In the $\epsilon = 13$ case, we find that $\nu = 4.37$ and the multiplicative constants are $c = 3.88$ for $\mathcal{V}_{pp\sigma}$ and $c = 4.46$ for $\mathcal{V}_{pp\pi}$. A larger rescaling power ν can easily be understood since less contrast produces less localized

TABLE I. The parameters for the ε elements.

	a_0	a_1	a_2	a_3	a_4
$\sqrt{\varepsilon_s}$	0.0804	0.0460	0.716	−0.0121	5.000
$\sqrt{\varepsilon_p}$	0.2371	0.0890	1.640	0.0020	0.320

TABLE II. The parameters for the V elements.

	b_1	b_2	b_3	c_1	c_2	c_3	c_4
$V_{ss\sigma}$	0.075	0.0008	10.0	−0.108	4.00	−0.000 96	1.30
$V_{pp\sigma}$	0.100	0.000 08	13.5	0.425	6.14	0.0550	3.22
$V_{pp\pi}$	0.700	0.0015	10.0	−0.076	5.40	−0.0044	2.32

resonances, and so the environmental effect will be larger. The rescaled $\mathcal{V}_{pp\sigma}$ and $\mathcal{V}_{pp\pi}$ are plotted in Figs. 3(c1) and 3(c2). We see that our TB parameters are transferable to other, more realistic, dielectric contrasts, with minor changes.

In conclusion, we have obtained a successful TB formulation of light propagation in 2D PBG structures with transferable matrix elements. Thus we provide an efficient scheme for handling not only periodic systems but defects and disordered cases as well. We hope that this scheme can be extended to 3D structures as well.

We thank C. Z. Wang and K. M. Ho for useful discussions. Ames Laboratory is operated for the U.S. Department of Energy by Iowa State University under Contract No. W-7405-Eng-82. This work was supported by the Director for Energy Research office of Basic Energy Sciences and Advanced Energy Projects, by NATO Grant No. 940647, by a ΠΕΝΕΔ grant, and by an EU grant.

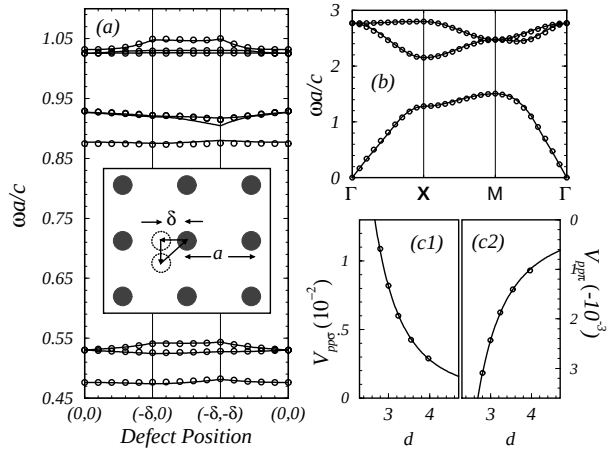

FIG. 3. (a) The three edge eigenfrequencies (circles for PWE, solid line for TB) for each band for a 3×3 supercell including a defect with $f = 20\%$. All cylinders are identical, with the middle one moving from the equilibrium position, as pointed in the inset graph with $\delta = a/4$. The wave vector is always constant $\vec{k}a = (0, 1/3)$. The first band gap extends approximately from $\omega a/c \simeq 0.53$ to $\omega a/c \simeq 0.87$, while the second starts at $\omega a/c \simeq 1.03$. (b) PWE bands (circles) along with the TB fit (solid line) for $\epsilon = 13$ and $f = 20\%$. (c) The fully rescaled $\mathcal{V}_{pp\sigma}$ [circles in (c1)] and $\mathcal{V}_{pp\pi}$ [circles in (c2)] for the system in (b) vs the dimensionless separation d. The solid line is the fit using the parameters from Table II and a multiplicative constant.

[1] (a) See, for example, *Photonic Band Gaps and Localization*, edited by C. M. Soukoulis (Plenum, New York, 1993); (b) J. Opt. Soc. Am. B **10**, 208–408 (1993); (c) *Photonic Band Gap Materials*, edited by C. M. Soukoulis (Kluwer, Dordrecht, 1996).

[2] J. Joannopoulos, R. D. Meade, and J. Winn, *Photonic Crystals* (Princeton University, Princeton, NJ, 1995).

[3] S. Datta, C. T. Chan, K. M. Ho, C. M. Soukoulis, and E. N. Economou, in *Photonic Band Gaps and Localization* [Ref. [1](a)], p. 289.

[4] M. Kafesaki, E. N. Economou, and M. M. Sigalas, in *Photonic Band Gap Materials* [Ref. [1](c)], p. 143.

[5] G. Mie, Ann. Phys. (Leipzig) **25**, 377 (1908); C. F. Bohren and D. R. Huffman, *Absorption and Scattering of Light by Small Particles* (J. Wiley, New York, 1983), Chap. 4.

[6] J. C. Slater and G. F. Koster, Phys. Rev. **94**, 1498 (1954).

[7] D. A. Papaconstantopoulos, *Handbook of the Electronic Structure of Elemental Solids* (Plenum Press, New York, 1986).

[8] W. A. Harrison, *Electronic Structure and the Properties of Solids* (Freeman, San Francisco, 1980).

[9] G. C. Fletcher, *The Electron Band Theory of Solids* (North-Holland Publishing Company, London, 1971).

[10] M. S. Tang, C. Z. Wang, C. T. Chan, and K. M. Ho, Phys. Rev. B **53**, 979 (1996).

[11] Note, however, that for $V_{pp\pi}$ matrix elements, since both lobes of the p resonance are involved, θ^1_{ilj} must take all possible values, but we will have to average over the contributions to each lobe. Also note that for the nonperiodic case, certain $H_{p_x p_y}$ and $H_{p_y p_x}$ matrix elements will not be complex conjugates if the formula is applied explicitly. In this event we have to average over the two possibilities, in order to keep the Hamiltonian matrix Hermitian.